Title
Bactericidal activity of gallium-doped chitosan coatings against staphylococcal infection

Journal
Journal of Applied Microbiology, 126(1)

ISSN
0021-8847

Authors
Esfahani, A Ghalayani
Lazazzera, B
Draghi, L
et al.

Publication Date
2019

DOI
10.1111/jam.14133

Peer reviewed

Title

Bactericidal activity of Gallium-doped chitosan coatings against staphylococcal infection

Authors

Arash Ghalayani Esfahani[1,3], Beth Lazazzera[2], Lorenza Draghi[3], Silvia Farè[3], Roberto Chiesa[3], Luigi De Nardo[3], Fabrizio Billi[1]

Affiliations

[1]Department of Orthopaedic Surgery, University of California, Los Angeles (UCLA), CA.

[2]Microbiology, Immunology, and Molecular Genetics Department, University of California, Los Angeles (UCLA), CA.

[3]Department of Chemistry, Materials and Chemical Engineering 'G. Natta', Politecnico di Milano, Milan, Italy.

Abbreviated running headline

Ga-doped CS coatings against staphylococcal infection

Corresponding author

Fabrizio Billi, Ph.D.
Professor
Co-Director, Orthopaedic Research at Harbor-UCLA Medical Center
UCLA/OIC Dept. of Orthopaedic Surgery
David Geffen School of Medicine, UCLABox 957358 Orthopaedic Hospital Research Center
615 Charles E. Young Dr. South, Room 450A
Los Angeles, CA 90095-7358

Office: 424-394-1832
Lab: 310-983-1035
Cell: 424-442-0364
Fax: 310-825-5409
email: f.billi@ucla.edu (PREFERRED)
fabrizio.billi@gmail.com

Abstract

Aims: This study was to develop a new class of Gallium (Ga)-doped Chitosan (CS) coatings fabricated by electrophoretic deposition (EPD) that promise new opportunities in staphylococcal infection therapy.

Methods and Results: Biofilm formation on EPD CS/Ga coatings by *Staphylococcus epidermidis* and *Staphylococcus aureus*, which are the main strains involved in post-arthroplasty infections was assessed. The codeposition of antibacterial agent was effective: Ga loaded into CS matrix reduces biofilm viability by up to 86% and 80% for *S. epidermidis* and *S. aureus* strains respectively. Lastly, the influence of Pulsed Electromagnetic Field (PEMF) on the bactericidal activity of CS/Ga coatings was investigated *in vitro*. To this end, the coatings were incubated with *S. epidermidis* and *S. aureus* and exposed to the PEMF using two different frequencies and times. Biofilm viability for *S. epidermidis* was decreased up to an additional 35 to 40% in the presence of low and high frequency PEMF, respectively. Biofilm viability by *S. aureus* was not further reduced in the presence of low frequency PEMF, but decreased up to an additional 38% at high frequency PEMF.

Conclusions: This study has established that a combination of pulsed electromagnetic fields with the antibacterial agent, improves bactericidal activity of Ga against *S. epidermidis* strain 14990 and *S. aureus* strain 12600.

Significance and Impact of the Study: The new integrated approach could reduce the incidence of infection in orthopaedic implant applications. It also clearly demonstrates that the combination of Ga treatment with PEMF could promise new opportunities in biofilm-associated infection therapy due to the improved Ga efficiency.

Keywords: electrophoretic deposition (EPD); chitosan (CS); gallium (Ga); *Staphylococcus epidermidis*; *Staphylococcus aureus*; post-arthroplasty infection; Pulsed Electromagnetic Field PEMF; biofilm.

Introduction

Infections after orthopaedic surgery has increased over the recent years despite the use of antibiotics and more refined surgical technique (Bozic and Ries 2005; Kurtz et al. 2008). As the demand for orthopaedic surgery increases with the aging population, the infection cases will pass 266,000 per year in the United States by 2030 (Bozic and Ries 2005; S. Kurtz et al. 2007; S. M. Kurtz et al. 2007; Kurtz et al. 2008). Bacteria (especially Staphylococci) form extracellular biofilms on implanted metallic/plastic materials, block penetration of immune cells and antibiotics, and result in bacterial survival (Darouiche 2004; Zimmerli et al. 2004; Trampuz and Widmer 2006; Del Pozo and Patel 2009). The surgical removal of all the implanted materials is necessary after biofilm formation. Near 70% of these kinds of infections are caused by Staphylococcal species (Fulkerson et al. 2006; Salgado et al. 2007; Walls et al. 2008). The pharmacological treatment of post-arthroplasty infection is difficult due to bacteria resistant to antibiotics such as methicillin-resistant S. *aureus* (MRSA) (Darouiche 2004; Zimmerli et al. 2004; Trampuz and Widmer 2006; Pulido et al. 2008; Del Pozo and Patel 2009). The conventional treatment for post-arthroplasty infection usually involves a two-stage procedure, first, surgical removal of all prosthetic components and placement of an antibiotic-impregnated spacer, and after, as the second step, revision arthroplasty after the infection has been cleared (Jiranek et al. 2006; Cui et al. 2007; Mittal et al. 2007; Diwanji et al. 2008; Chiu and Lin 2009; Toulson et al. 2009). Togherther with the patient disconfort, this additional procedures care result in additional medical costs. All these issues lead to focus on the prevention of infection (Campoccia et al. 2006; Hetrick and Schoenfisch 2006; Zhao et al. 2009).

As a novel method to tackle this issue, we designed Chitosan (CS)/gallium (Ga) composite coating to be applied to implant surfaces, prepared by electrophoretic deposition (EPD). EPD is a deposition technique with different advantages such as cost-effectiveness, versatility in materials that can be processed, reasonable control over the thickness of the coatings and a high level of homogeneity in terms of microstructure (Besra and Liu 2007). Chitosan is a

cationic polysaccharide biopolymer for tissue engineering, as it is a biocompatible coating and capable of drug delivery (Simchi et al. 2009). According to the particular CS properties such as biodegradability, biocompatibility, non-toxicity, it is one of the most interesting materials for tissue engineering ranging from skin, bone, cartilage, and vascular grafts as substrates for cell culture and drug-delivery systems (Malafaya et al. 2007). Previous studies have shown the feasibility of cationic EPD of chitosan (Varoni et al. 2016). Ga(III) can be potentially used as an antibacterial agent. As Ga^{3+} is similar to Fe^{3+} in radius, electronegativity, charge and coordination number (da Silva et al. 2009; Franchini et al. 2012), it can substitute the iron in its process and act as "Trojan horse" against bacteria, such as *Pseudomonas aeruginosa* and *Staphylococcus epidermidis* (Kaneko et al. 2007; Rzhepishevska et al. 2011). Ga is sequestered by the bacteria through their iron uptake systems, by the siderophores. Once inside, the metal blocks iron-dependent process where there is crucial oxidation of iron (Fe^{2+} to Fe^{3+}) because gallium III cannot be reduced to give continuity to sequential oxidation and reduction (da Silva et al. 2009). Ga(III) blocks osteoclast resorption by preventing attachment to the surface of bone without appearing to be cytotoxic to osteoclasts, nor to inhibit cellular metabolism (Rimondini et al. 2013; Cochis et al. 2016).

In this work, after studying the morphology of the coatings and finding the optimum conditions for uniform coating, the release profile of Ga in different concentrations were studied, as Ga results in bactericidal activity. We assessed biofilm formation and cell growth in the presence of the composite-coated surfaces by *Staphylococcus epidermidis and Staphylococcus aureus,* both Gram-positive bacteria, which are the two main strains that cause post-arthroplasty infections (Campoccia et al. 2006; Del Pozo and Patel 2009; Lv et al. 2014). For this reason, this work studied antibacterial activity of EPD of CS/Ga composite coatings against Gram-positive bacteria.

The electrophoretic deposition of CS/Ga coating on orthopaedic implants show excellent bactericidal activity as well as biocompatible properties. Furthermore, the polymer-antibacterial agent (Ga) implant coating evaluated in this study was effective, suggesting the

potential for this strategy as a therapeutic intervention to combat post-arthroplasty infections. This novel coating could reduce the incidence of infection in orthopaedic implant applications. Finally, the *in vitro* influence of Pulsed Electromagnetic Field (PEMF) is investigated on modification of bactericidal activity of the CS/Ga composite coatings. The thera- peutic efficacy for the stimulation of bone growth with pulsating electromagnetic fields (PEMF) is already proven in controlled double-blind studies (Sharrard 1990; Linovitz et al. 2002; Simonis et al. 2003; Griffin et al. 2008). The PEMF resulted in a further decrease in biofilm viability up to 40% for *S. epidermidis* and 38% for *S. aureus* compared to Ga treatment alone.

Materials and methods

Materials

Chitosan (Deacetylated chitin, Poly(D-glucosamine), medium molecular weight, Lot#STBG1894V), Gallium(III) nitrate hydrate (crystalline, 99.9% trace metals basis, Lot#MKBQ1999V), acetic acid (99.7%), Dulbecco's Phosphate Buffered Saline (DPBS) (Lot#RNBG5989), lysozyme from chicken egg white (Lot#SLBX2243) and water (CHROMASOLV® Plus, for HPLC) were all supplied by Sigma-Aldrich and used without further purification. To evaluate the in vitro biological response, human primary osteogenic sarcoma cell line SAOS-2 (ECACC 89050205) was used.

Trypticase soy broth (TSB) (30 g L^{-1} in purified water, autoclave at 121 ^{o}C for 15 minutes, Becton, Dickinson and Company) was used for routine growth of bacterial cells, crystal violet stain was used to quantify biofilm viability (0.41% W/V in ethanol and DI water, Fisher scientific company), and Wash Buffer was used to change the medium of the bacterial cells (Hamon and Lazazzera 2002).

Staphylococcus epidermidis strain 14990 and *Staphylococcus aureus* strain 12600 both from the American Type Culture Collection (ATCC) were used in the study.

Preparation and chemico-physical characterization of CS/Ga composite coating

EPD of CS/Ga composite coating

Titanium sheets (Ti, grade 2) were used as cathode in an electrophoretic deposition cell: electrodes were positioned at distance of 10 mm (Isfahani and Ghorbani 2013) in a lab made EPD cell. Processing conditions have been optimized in order to achieve a uniform, homogeneous and consistant deposition of coatings; Square waves (75-100 V, duty cycle = 0.17) have been used in water-based bath (pH=3.67, [CS] = 1g L^{-1}, [Gallium(III) nitrate hydrate] = 10 mg L^{-1} (LGa) and [Gallium(III) nitrate hydrate] = 100 mg L^{-1} (HGa)).

Microstructural characterization

In the first phase, the feasibility of coating with Inductively Coupled Plasma - Optical Emission Spectrometry (ICP-OES, Perkin Elmer Optima 2000DV OES, Wellesley, USA) technique was evaluated. In order to study the morphology of CS/Ga composite coating prepared by EPD, scanning electron microscope (SEM) (Zeiss EVO 50EP) was used. To prepare the obtained samples for SEM, specimens were washed 3 times in de-ionized water before overnight lyophilizing. The SEM was equipped with an Oxford Instruments INCA energy-dispersive X-ray spectrometer (EDS) for qualitative elemental analysis of the coatings. To measure the conductivity of deposition bath, conductivity meter (Crison, CM 35) has been used.

In vitro degradation

The degradation study was performed by immersing the specimens in Phosphate Buffer Solution (PBS) (pH 7.4) at 37 °C containing 1.5 μg ml^{-1} lysozyme (from chicken egg white). The lysozyme concentration was selected according to the concentration in human serum (Brouwer et al. 1984; Porstmann et al. 1989). The dried scaffolds were cut into small circles specimens (D=7 mm) and weighed (dry weight). At different time points (up to 3 D), specimens were removed from the solution and carefully dried in 37 °C oven overnight. The specimens were weighted to measure the weight loss:

$$\text{Weight loss (\%)} = \frac{Wt-Wo}{W0} * 100 \qquad \text{(Equation 1)}$$

Where the w_t is the weight of dry specimen at different time points, w_o is the weight of dry specimen before immersing in lysozyme solution.

Antibacterial agent (Ga) release study

The in vitro release of Ga from the EPD chitosan matrix was studied by incubating composite coating (20 mm × 20 mm × 0.2 mm) in 7.5 mL of phosphate buffered saline (PBS, Sigma-Aldrich P4417-50TB) at 37 °C. Inductively Coupled Plasma - Optical Emission Spectrometry

(ICP-OES, Perkin Elmer Optima 2000DV OES, Wellesley, USA) analysis was used to investigate the release of antibacterial agent. To determine release of Ga from the CS matrix, 3 specimens for each treatment at each time point (1, 2, 4, 8, 14, 24 hours and 3, 7 days) were incubated in PBS. They were fixed vertically in 15 mL falcon tubes with conical end, to allow release of the antibacterial agent from both sides of the specimen. The tubes were maintained at 37 °C in a thermostatic oven under constant gentle shaking (75 rpm) (VDRL DIGITAL MOD. 711/D). Aliquots of PBS from three specimens was analyzed by ICP-OES to determine the concentration of Ga released. The PBS solution was also analyzed by ICP-EOS to standardize the data.

Biological and microbiological characterization

Cytotoxicity tests on extract

For cytotoxicity assessment, samples eluates were obtained, according to UNI EN ISO 10993-5, by incubating the samples in culture medium for 24 h. Cell culture medium was prepared using McCoy's 5a medium, with 15% fetal bovine serum, 1% [v/v] L-glutamine 2 mM, 1% [v/v] sodium pyruvate 1 mM and 1% [v/v] penicillin/streptomycin.

The extraction ratio (sample surface area/eluates volume) was 3 cm^2 mL^{-1}. SAOS-2 cells were seeded at a density of 10^4 cells cm^{-2} in 96-well microtiter plate and cultured with complete medium until 70% confluent for 24 h. The medium was then replaced with eluates or control (i.e. 24 hours old medium) and cells were returned to incubator. After 24 h, Alamar Blue™ assay (BioReagent, Sigma-Aidrich R7017) was performed to evaluate cell viability. Plates fluorescence (530 nm_{EX}/590 nm_{Em}) was spectrophotometrically read (Tecan, Genios Plus plate reader) to evaluate possible cytotoxic effects associated to the tested material.

Crystal violet assay and colony-forming units counting

To evaluate biofilm viability by *S. epidermidis* and *S. aureus*, crystal violet assay was performed. A 1 ml of diluted (1:100) overnight culture of *S. epidermidis* in TSB was added to each sample in each well of 24 well, flat bottom microtitre plate. All the coatings autoclaved

(Tuttnauer cat2007) for 1 hour in 150 °C to be sterilized. The plate was incubated under static conditions at 37 °C for 24 hours. The growth media removed, and the wells washed 3 times with 1 ml Wash Buffer. At the next step, 1 ml crystal violet was added to each well and incubated at room temperature for 15 minutes. Crystal violet was removed, and the wells were washed twice with 1 ml of distilled water and 1 ml of an 80% ethanol, 20% acetone solution was added. The liquid was transferred to a fresh 96 well PVC round bottom microtiter plate to measure the absorbance at 570 nm (A_{570}) by plate reader (BMG FLUOstar Omega). Control is CS coating without any Ga.

Biofilm viability (%) = $\frac{Composite\ coating Ab_s}{Control\ Ab_s}$ x 100 (Equation 2)

To allow the biofilm to detach from the coating surface, coating containing biofilms were resuspended in 1 mL of TSB, vortexed, and sonicated at 60 Hz (Aquasonic 250HT, VWR International) for 30 s; this was repeated five times. The suspension was used to prepare six, ten-fold dilutions. A 100 µL volume of each dilution were spotted onto Lysogeny broth (LB) plates and incubated for 24 h at 37 °C. The following day, the number of CFUs per ml was counted, working blind, and using the following formula (Kuhn et al. 2003; Harrison et al. 2006; Rivardo et al. 2009):

CFU ml^{-1} = (no. of colonies x dilution factor) / volume of culture plate. (Equation 3)

Biofilm morphology

To study the morphology of biofilm which was formed by *S. epidermidis* on the CS/Ga coatings, Variable-Pressure (VP) Scanning Electron Microscopy (SEM) (Zeiss supra 40VP) was used. The samples were washed 3 times in de-ionized water and dried in 37 °C oven for 1h.

Pulsed electromagnetic field (PEMF)

To investigate the in vitro effect of a pulsed electromagnetic field (PEMF) on the efficacy of antibacterial agent (Ga) in the treatment of coated orthopaedic implants infection, two different frequencies, 40,850 Hz as the high frequency and 3,846 Hz as the low frequency, were used

to expose the specimens to the PEMF. PEMF was applied for 15 minutes and 4 hours to the coatings which were incubated into *S. epidermidis* strain 14990 and *S. aureus* strain 12600 in 24 well microtiter rack. The rack was located in the incubator. The Dial-A-Stim IV (DAS-IV) in vitro system used to generate PEMF for the experiments.

The Dial-A-Stim IV (DAS-IV) in vitro system used to generate PEMF for the experiments. It consists of equipment and a treatment rack capable of providing low frequency (LF) and high frequency (HF) Physio-Stim treatment for different levels of in vitro test samples. The system components are treatment rack, control box, arbitrary waveform generator and treatment timer and reset/start button. Treatment rack which consists of four levels is shown in Figure 2. The purpose of arbitrary waveform generator is to configure the control signals used to generate the PEMF waveform by the module driver. The signals will be sent to the treatment rack by the control box.

Statistical data analysis

All results are reported as mean ± standard deviation. Significant differences between two sets of data were determined by one-way ANOVA followed by Tukey post-hoc test for pairwise comparisons and $p < 0.05$ was considered statistically significant. The Statistical Package for Social Science was used for the calculations (Minitab Express™ Version 1.4.0).

Results

Feasibility of EPD CS/Ga composite coating

Figure 3 shows the SEM images of (a) pure CS and (b,c) CS/Ga composite coating with different Ga concentrations ([Gallium(III) nitrate hydrate] = 10 and 100 mg L^{-1}): a porous structure in pure CS coating is evident. Ga-doped coatings show a different morphology and an homogeneous presence of bright spots. Energy-dispersive X-ray (EDX) analysis allow the identification of such clusters, mainly deposited on the pore borders (Figure 3 d,e). The EDX spectrum (Figure 3(f,g)) contains peaks associated with Ga atoms.

Before studying the Ga release rate, the total amount of Ga loaded in the chitosan matrix during EPD was determined as a function of Ga content in the suspension by ICP-OES analysis (Figure 4a). As seen, the efficiency during EPD was approximately 66-55% which is quite acceptable (Figure 4a) (supporting information).

The release of Ga from CS matrix, measured by ICP-EOS, occurred during the first 7 days. The released Ga was detected in 7.5mL of PBS with a maximum of 0.0137 and 0.0013 mg cm^{-2} from high Ga concentration ([Gallium(III) nitrate hydrate] = 100 mg L^{-1}) and low Ga concentration ([Gallium(III) nitrate hydrate] = 10 mg L^{-1}) deposition baths, respectively (Figure 4b).

To evaluate whether the release rate is controlled by degradation of the chitosan matrix in the PBS solution over long incubation, the cumulative weight loss of the CS coating in PBS was also determined (Figure 4c). As it can be observed, the amount of chitosan weight loss in PBS was noticeable only after a long period of incubation.

Degradation

Figure (5) summarized the biodegradation results. An increasing weight loss observed for CS and CS/Ga composite coatings in the course of time. CS sample showed 34.2% degradation

whitin 3 days. This number is 21.4% and 19.8% for CS/LGa and CS/HGa composite structure respectively.

Cytotoxicity assessment and bactericidal activity

Cytotoxicity - test on extracts

Figure (6) shows the results of cell viability for SAOS-2 cells cultured with pure (100%) or diluted (50% and 10% in fresh medium) eluates from CS and CS/Ga composite coatings. No evidence of cytotoxicity was detected in any of the examined samples. The cell viability (%) vs. control was 109.76%, 107.77% and 96.05% for CS, CS/LGa and CS/HGa composite coatings, respectively.

Biofilm viability

Figure 7 a and 8 a summarizes the biofilm viability results assayed by the crystal violet method on *S. epidermidis* strain 14990 and S. *aureus* strain 12600, cultured in TSB medium. After 24h, all Ga-doped specimens differed significantly from untreated pure CS coating ($p < 0.05$, figure 7 and 8, indicated by *) resulting in a significant bacterial inhibition. For *S. epidermidis*, both CS/LGa and CS/HGa coatings caused a reduction in biofilm viability of about 15% and 60%, respectively, after 24 hrs, and a reduction of 82% and 86%, respectively, after 3 days (Figure 7a). For *S. aureus*, both CS/LGa and CS/HGa coatings caused a reduction in biofilm viability of about 10% and 55%, respectively, after 24 hrs, and a reduction of 40% and 80%, respectively, after 3 days (Figure 8a) due to the Ga released amount increasement.

This assay was repeated with TSB media adjusted to different pHs; regardless of the medium pH the CS/Ga coated reduced in the number of viable bacterial cells (Figure 7b and 8b).

The effect of the CS/Ga composite coating on cell viability of *S. epidermidis* was measured as the total CFU present in the plantonic phase of the cultures incubated with the coatings (Figure 9). The composite coating with a high Ga concentration (HGa) gave the lowest number of planktonic CFU, yeilding. 8.3% and 4.5% of the population on untreated CS after 24 hours

and 3 days, respectively. The effect of the CS/Ga compositie coating of the viability of cells in the biofilm phase of the culture was measured as the total CFU presence in the medium after detachment of the cells from the surface. The coatings with highest Ga concentration resulted in the lowest CFU, yielding 27% and 37% of the population on untreated CS for *S. epidermidis* strain 14990 and *S. aureus* strain 12600, respectively (Figure 10).

Biofilm morphology

At different Ga concentration, colonies were attached on the surface of the coating specimen over 24h incubation. These results were substantiated by the VP-SEM images (Figure 11 and 12). The SEM micrographs revealed reduced biofilm formation by *S. epidermidis* and *S. aureus* grown on CS/Ga composite coatings compared with the pure CS control (Figure 11a and 12a). The biofilm formed on Ga were poorly structured, very thin, arrested at the microcolony stage, and had reduced surface area coverage. It is also evident that the biofilm structure on the CS/HGa composite coating (Figure 11c and 12c) is only a single-layer of cells compare to CS/LGa composite structure biofilm (Figure 11b and 12b).

PEMF effect on bactericidal activity of the coatings

Four separate experimental setups were used to expose coatings incubated in bacterial cultures of *S. epidermidis* and *S. aureus* in TSB media, to (1) a low-frequency PEMF, 3,846 Hz for 15 minutes and 4 h and (2) a hi-frequency PEMF, 40,850 Hz for 15 minutes and 4 h as well. In each of the four applied fields showed a biofilm viability reduction of *S. epidermidis and S. aureus* in the presence of Ga within 24 h of the experiment (Figure 13 and 14). The best results were obtained by low frequency for 4 h in both strains. Exposure to a PEMF increased the effectiveness of Ga against the one-day biofilms of *S. epidermidis* and *S. aureus*.

Discussion

After fabricating CS/Ga composite coating by EPD, its feasibility was confirmed by X-ray map and EDX spectrum techniques and due to hydrolysis of water during EPD process (Varoni et al. 2016), a porous structure in pure CS is evident. Ga appears distributed mainly on pore bordes, probably due to the higher current density in such area (Lanzi 1990; Zhitomirsky and Gal-or 1997; Besra and Liu 2007). From EDX analysis a difference is evident in the relative peak of Ga according to the different bath concentrations.

EDX analysis performed on chitosan/Ga substrates proved the presence of gallium (Figure 3f – 3g) as well as the ICP-OES investigation detected the Ga release from the prepared materials (Figure 4a). This result highlights that gallium could be physically bonded to chitosan macromolecules (e.g., weak bonds) or entrapped into the chitosan macromolecules (supporting information S.2- Figure S.1).

The degradation of chitosan has already been studied carefully before (Pangburn et al. 1982; Lee et al. 1995; Tomihata and Ikada 1997; Vårum et al. 1997). In general, polysaccharides are degraded by enzymatic hydrolysis. It is well established that, in human serum, chitosan is depolymerized enzymatically by lysozyme (Vårum et al. 1997). The enzyme hydrolyzes the glycosidic bonds of polysaccharide which results in biodegradation. Lysozyme contains a hexameric binding site (Pangburn et al. 1982), and hexasaccharide chains containing acetylated units lead to initial degradation of the CS and CS/Ga composite coatings (Nordtveit et al. 1994).

The critical period to inhibit biofilm formation after the implantation surgery is 6 h (Zilberman and Elsner 2008). However, even at longer term, certain species of adhered bacteria are capable of forming a biofilm at the implant–tissue interface (Hetrick and Schoenfisch 2006; Zilberman and Elsner 2008; Simchi et al. 2011). Therefore, we performed the drug release studies for an extended time period. Two release phases can be highlighted. In the early phase, a burst of release was observed (after 2h). A second phase follows, in which very little additional release was detected. Significant CS weight loss was observed only after a long

362 period of incubation in PBS (Ordikhani et al. 2014), suggesting that water molecules destroy
363 the hydrogen bond among chitosan fibers, disordering the macromolecule alignments that
364 may lead to dissolution/degradation.
365 As a prerequisite, the cytotoxicity assessment suggests that the prepared composite coatings
366 are not toxic to human osteoblabst-like cells in good agreement with previous studies (Cochis
367 et al. 2016).
368 To evaluate bactericidal activity of CS/Ga coatings different aspects should be considered.
369 First of all, CS inherently shows remarkable antibacterial activity against a broad spectrum of
370 bacteria due to the interaction between positively charged CS and negatively charged
371 microbial cell wall, which leads to the leakage of intracellular constituents (Aimin et al. 1999;
372 Kim et al. 2008). Another phenomenon that should be considered is pH-responsive swelling
373 behavior of chitosan which makes CS to be a proper matrix for controlled release of
374 pharmaceuticals (Aimin et al. 1999). In the following, the biofilm viability assay in different pHs
375 on *S. epidermidis* strain 14990 and *S. aureus* strain 12600 is discussed. Generally, the pH
376 drops in presence of bacteria (Bernthal et al. 2010) CS matrix was confirmed to release Ga
377 both passively and actively, in response to lowering pH. At lower pH, the amide groups on the
378 chitosan can become protonated, forming the hydrophilic NH_3^+ group. The resulting
379 electrostatic repulsion between the protonated amino groups weakened the intermolecular
380 and intramolecular hydrogen bonding interaction of chitosan molecules, as a result, the buffer
381 solution can diffuse into the network easily which would facilitate the equilibrium swelling ratios
382 to increase. According to the swelling, the diffusion rate increases from matrix to the exterior.
383 As a consequence the embeded agents in the matrix will be released easier and faster (Zou
384 et al. 2015).
385 Besides affecting planktonic bacteria, Ga seems to be efficient to reduce biofilm cells (Figure
386 10). Consequently, Ga, can be effective against either planktonic or biofilm cells. Gallium is
387 metabolically very similar to Fe^{3+}, acting as an iron substitute in several biological pathways.
388 Respect to its chemical similarity to Fe^{3+} in terms of charge, ionic radius, electronic

389 configuration, and coordination number, Ga can substitute iron in siderophore dependent
390 biological systems; this capability underlies its antibacterial action. Since Ga^{3+} cannot be
391 reduced under the same conditions as Fe^{3+}, sequential redox reactions critical for the
392 biological functions by Fe^{3+} are impaired when iron is replaced: Ga thus inhibits Fe^{3+} by a
393 “Trojan horse” strategy (Kaneko et al. 2007; García-Contreras et al. 2014; Modarresi et al.
394 2015).
395 As previusly mentioned, the thera-peutic efficacy for the stimulation of bone growth with
396 pulsating electromagnetic fields (PEMF) is already proven. Recently, enhancing the
397 eradication of biofilms in the clinical infection of implants is being viewed with more interest.
398 For the first time, Khoury et al, demonstrated that antibiotics efficacy would be increased
399 against biofilm bacteria in the presence of very week electric field (Khoury et al. 1992).
400 Growth inhibition of *S. aureus* induced by low-frequency electric and electromagnetic fields
401 also reported by Obermeier et al (Obermeier et al. 2009).
402 The PEMF resulted in a further decrease in biofilm viability up to 40% for S. epidermidis and
403 38% for S. aureus compared to Ga treatment alone.
404 However, Reactive oxygen and Nitrogen Species (ROS/RNS) were not measured in the
405 medium after magnetic treatment, according to the PEMF effect on bactericidal activity of the
406 obtained CS/Ga coatings results, hydroxyl and oxygen radicals are known to destroy cell
407 membranes of bacteria and may be present with the application of an electromagnetic field.
408 This is the so-called bioelectric effect (Benson et al. 1994; Costerton et al. 1994; McLeod et
409 al. 1999; Pickering et al. 2003). This may facilitate the penetration of antibacterial agents into
410 the biofilm and subsequently in the cells and could be an explanation for the detected
411 modification of Ga efficacy.
412 In this study, we have demonstrated that a combination of pulsed electromagnetic fields with
413 the antibacterial agent, improves bactericidal activity of Ga against *S. epidermidis* strain 14990
414 and *S. aureus* strain 12600. We conclude that the combination of Ga treatment with low-

frequency PEMF could promise new opportunities in biofilm-associated infection therapy due to the improved Ga efficiency.

Taken together, an animal model could be potentially be used to provide important information about *in vivo* clinical efficacy of preclinical preventative or therapeutic modalities against post-arthroplasty infections before more extensive studies in human subjects. Furthermore, the therapeutic efficacy of the Ga under the used fields, should be proven in well-designed, evidence-based, randomized clinical studies in the future. PEMF can be developed into a device that can be applied externally to patients. This novel modification could result in the lower antibacterial agent use which decreases the health side effects.

Acknowlegement

AGE and LDN would like to thank Dario Picenoni (RIP) for providing the morphology SEM micrographs.

Conflict of Interest

The authors of the study declare there are no known competing interests associated with this study or the data contained within.

References

Aimin, C. et al. 1999. Antibiotic Loaded Chitosan Bar: An In Vitro, In Vivo Study of a Possible Treatment for Osteomyelitis. *Clin Orthop Relat Res* ® 366.

Benson, D.E. et al. 1994. Magnetic field enhancement of antibiotic activity in biofilm forming Pseudomonas aeruginosa. *ASAIO J (1992)* 40(3), pp. M371-6.

Bernthal, N.M. et al. 2010. A Mouse Model of Post-Arthroplasty Staphylococcus aureus Joint Infection to Evaluate In Vivo the Efficacy of Antimicrobial Implant Coatings. Planet, P. J. ed. PLoS ONE 5(9), p. e12580.

Besra, L. and Liu, M. 2007. A review on fundamentals and applications of electrophoretic deposition (EPD). *Prog Mater Sci* 52(1), pp. 1–61. doi: 10.1016/j.pmatsci.2006.07.001.

Bozic, K.J. and Ries, M.D. 2005. THE IMPACT OF INFECTION AFTER TOTAL HIP ARTHROPLASTY ON HOSPITAL AND SURGEON RESOURCE UTILIZATION. *J Bone Joint Surg* 87(8).

Brouwer, J. et al. 1984. Determination of lysozyme in serum, urine, cerebrospinal fluid and feces by enzyme immunoassay. *Clin Chim Acta* 142(1), pp. 21–30.

Campoccia, D. et al. 2006. The significance of infection related to orthopedic devices and issues of antibiotic resistance. *Biomaterials* 27(11), pp. 2331–2339.

Chiu, F.-Y. and Lin, C.-F.J. 2009. Antibiotic-Impregnated Cement in Revision Total Knee Arthroplasty. *J Bone Joint Surg Am Volume* 91(3), pp. 628–633.

Cochis, A. et al. 2016. Biomaterials The effect of silver or gallium doped titanium against the multidrug resistant Acinetobacter baumannii. *Biomaterials* 80, pp. 80–95.

Costerton, J.W. et al. 1994. Mechanism of electrical enhancement of efficacy of antibiotics in killing biofilm bacteria. *Antimicrob Agents Chemother* 38(12), pp. 2803–9.

Cui, Q. et al. 2007. Antibiotic-Impregnated Cement Spacers for the Treatment of Infection Associated with Total Hip or Knee Arthroplasty. *J Bone Joint Surg* 89(4).

Darouiche, R.O. 2004. Treatment of Infections Associated with Surgical Implants. *N Engl J Med* 350(14), pp. 1422–1429.

Diwanji, S.R. et al. 2008. Two-stage reconstruction of infected hip joints. *J Arthroplasty* 23(5), pp. 656–61.

Franchini, M. et al. 2012. Gallium-containing phospho-silicate glasses: Synthesis and in vitro bioactivity. *Mater Sci Eng: C* 32(6), pp. 1401–1406.

Fulkerson, E. et al. 2006. Antibiotic Susceptibility of Bacteria Infecting Total Joint Arthroplasty Sites. *J Bone Joint Surg* 88(6), pp. 1231–1237.

García-Contreras, R. et al. 2014. Gallium induces the production of virulence factors in *Pseudomonas aeruginosa*. *Pathog Dis* 70(1), pp. 95–98.

Griffin, X.L. et al. 2008. The role of electromagnetic stimulation in the management of established non-union of long bone fractures: What is the evidence? *Injury* 39(4), pp. 419–429.

Hamon, M.A. and Lazazzera, B.A. 2002. The sporulation transcription factor Spo0A is required for biofilm development in Bacillus subtilis. *Mol Microbiol* 42(5), pp. 1199–1209.

Harrison, J.J. et al. 2006. The use of microscopy and three-dimensional visualization to evaluate the structure of microbial biofilms cultivated in the calgary biofilm device. *Biol Proced Online* 8(1), pp. 194–215.

Hetrick, E.M. and Schoenfisch, M.H. 2006. Reducing implant-related infections: active release strategies. *Chem Soc Rev* 35(9), p. 780.

Isfahani, A.G. and Ghorbani, M. 2013. Electrophoretic Deposition of Ni/SiO2 Nanocomposite Coating: Fabrication Process and Tribological and Corrosion Properties. *J Nano R* 26, pp. 45–51.

Jiranek, W.A. et al. 2006. Antibiotic-Loaded Bone Cement for Infection Prophylaxis in Total Joint Replacement. *J Bone Joint Surg* 88(11), pp. 2487–2500.

Kaneko, Y. et al. 2007. The transition metal gallium disrupts Pseudomonas aeruginosa iron metabolism and has antimicrobial and antibiofilm activity. *J Clin Invest* 117(4), pp. 877–88.

Khoury, A.E. et al. 1992. Prevention and control of bacterial infections associated with medical devices. *ASAIO J (1992)* 38(3), pp. M174-8.

Kim, I.-Y. et al. 2008. Chitosan and its derivatives for tissue engineering applications. *Biotechnol Adv* 26(1), pp. 1–21.

Kuhn, D.M. et al. 2003. Uses and limitations of the XTT assay in studies of Candida growth and metabolism. *J Clin Microbiol* 41(1), pp. 506–8.

Kurtz, S. et al. 2007. Projections of Primary and Revision Hip and Knee Arthroplasty in the United States from 2005 to 2030. *J Bone Joint Surg* 89(4).

Kurtz, S.M. et al. 2007. Future Clinical and Economic Impact of Revision Total Hip and Knee Arthroplasty. 89.

Kurtz, S.M. et al. 2008. Infection burden for hip and knee arthroplasty in the United States. *J Arthroplasty* 23(7), pp. 984–91.

Lanzi, O. 1990. Effect of Pore Structure on Current and Potential Distributions in a Porous Electrode. *J Electrochem Soc* 137(2), p. 585. doi: 10.1149/1.2086511.

Lee, K.Y. et al. 1995. Blood compatibility and biodegradability of partially N-acylated chitosan derivatives. *Biomaterials* 16(16), pp. 1211–1216.

Linovitz, R.J. et al. 2002. Combined Magnetic Fields Accelerate and Increase Spine Fusion: A Double-Blind, Randomized, Placebo Controlled Study. *Spine* 27(13).

Lv, H. et al. 2014. Layer-by-layer self-assembly of minocycline-loaded chitosan/alginate multilayer on titanium substrates to inhibit biofilm formation. *J Dent* 42(11), pp. 1464–1472.

Malafaya, P.B. et al. 2007. Natural-origin polymers as carriers and scaffolds for biomolecules and cell delivery in tissue engineering applications. *Adv Drug Deliv Rev* 59(4–5), pp. 207–233. doi: 10.1016/j.addr.2007.03.012.

McLeod, B.R. et al. 1999. [49] Enhanced bacterial biofilm control using electromagnetic fields in combination with antibiotics. *Methods Enzymol* 310, pp. 656–670.

Mittal, Y. et al. 2007. Two-Stage Reimplantation for Periprosthetic Knee Infection Involving Resistant Organisms. *J Bone Joint Surg* 89(6), pp. 1227–1231.

Modarresi, F. et al. 2015. Iron limitation enhances acyl homoserine lactone (AHL) production and biofilm formation in clinical isolates of *Acinetobacter baumannii*. *Virulence* 6(2), pp. 152–

161.

Nordtveit, R.J. et al. 1994. Degradation of fully water-soluble, partially N-acetylated chitosans with lysozyme. *Carbohydr Polym* 23(4), pp. 253–260.

Obermeier, A. et al. 2009. Growth inhibition of *Staphylococcus aureus* induced by low-frequency electric and electromagnetic fields. *Bioelectromagnetics* 30(4), pp. 270–279.

Ordikhani, F. et al. 2014. Characterization and antibacterial performance of electrodeposited chitosan-vancomycin composite coatings for prevention of implant-associated infections. *Mater Sci Eng: C* 41, pp. 240–248.

Pangburn, S.. et al. 1982. Lysozyme degradation of partially deacetylated chitin, its films and hydrogels. *Biomaterials* 3(2), pp. 105–108.

Pickering, S.A.W. et al. 2003. Electromagnetic augmentation of antibiotic efficacy in infection of orthopaedic implants. *J Bone Joint Surg Br volume* 85–B(4), pp. 588–593.

Porstmann, B. et al. 1989. Measurement of lysozyme in human body fluids: Comparison of various enzyme immunoassay techniques and their diagnostic application. *Clin Biochem* 22(5), pp. 349–355.

Del Pozo, J.L. and Patel, R. 2009. Infection Associated with Prosthetic Joints. *New England J Med* 361(8), pp. 787–794.

Pulido, L. et al. 2008. Periprosthetic Joint Infection: The Incidence, Timing, and Predisposing Factors. *Clin Orthop Relat Res* 466(7), pp. 1710–1715.

Rimondini, L. et al. 2013. The Biofilm Formation onto Implants and Prosthetic Materials May Be Contrasted Using Gallium (3+). *Key Eng Mater* 587, pp. 315–320..

Rivardo, F. et al. 2009. Anti-adhesion activity of two biosurfactants produced by Bacillus spp. prevents biofilm formation of human bacterial pathogens. *Appl Microbiol Biotechnol* 83(3), pp. 541–553.

Rzhepishevska, O. et al. 2011. The antibacterial activity of Ga3+ is influenced by ligand complexation as well as the bacterial carbon source. *Antimicrob Agents Chemother* 55(12), pp. 5568–80.

Salgado, C.D. et al. 2007. Higher Risk of Failure of Methicillin-resistant Staphylococcus aureus Prosthetic Joint Infections. *Clin Orthop Relat Res* PAP.

Sharrard, W.J. 1990. A double-blind trial of pulsed electromagnetic fields for delayed union of tibial fractures. *J Bone Joint Surg Br* 72(3), pp. 347–55.

da Silva, J.G. et al. 2009. Increasing the antibacterial activity of gallium(III) against Pseudomonas aeruginosa upon coordination to pyridine-derived thiosemicarbazones. *Polyhedron* 28(11), pp. 2301–2305.

Simchi, A. et al. 2009. Electrophoretic deposition of chitosan. *Mater Lett* 63(26), pp. 2253–2256.

Simchi, A. et al. 2011. Recent progress in inorganic and composite coatings with bactericidal capability for orthopaedic applications. *Nanomedicine* 7(1), pp. 22–39.

Simonis, R.B. et al. 2003. Electrical treatment of tibial non-union: a prospective, randomised, double-blind trial. *Injury* 34(5), pp. 357–62.

Tomihata, K. and Ikada, Y. 1997. In vitro and in vivo degradation of films of chitin and its deacetylated derivatives. *Biomaterials* 18(7), pp. 567–575.

Toulson, C. et al. 2009. Treatment of Infected Total Hip Arthroplasty With a 2-Stage Reimplantation Protocol: Update on “Our Institution's” Experience From 1989 to 2003. *J Arthroplasty* 24(7), pp. 1051–60.

Trampuz, A. and Widmer, A.F. 2006. Infections associated with orthopedic implants. *Curr Opin Infect Dis* 19(4), pp. 349–356.

Varoni, E.M. et al. 2016. Hierarchic micro-patterned porous scaffolds via electrochemical replica-deposition enhance neo-vascularization. *Biomed Mater* 00(January), pp. 1–13.

Vårum, K.M. et al. 1997. In vitro degradation rates of partially N-acetylated chitosans in human serum. *Carbohydr Res* 299(1–2), pp. 99–101.

Walls, R.J. et al. 2008. Surgical site infection with methicillin-resistant *Staphylococcus aureus* after primary total hip replacement. *J Bone Joint Surg Br volume* 90–B(3), pp. 292–298.

Zhao, L. et al. 2009. Antibacterial coatings on titanium implants. *J Biomed Mater Res B*

567 91(1), pp. 470–480. doi: 10.1002/jbm.b.31463.
568 Zhitomirsky, I. and Gal-or, L. 1997. Electrophoretic deposition of hydroxyapatite. *J Mater Sci*
569 *Mater Med* 8(4), pp. 213–219.
570 Zilberman, M. and Elsner, J.J. 2008. Antibiotic-eluting medical devices for various
571 applications. *J Control Release* 130(3), pp. 202–215.
572 Zimmerli, W. et al. 2004. Prosthetic-Joint Infections. *N Engl J Med* 351(16), pp. 1645–1654.
573 Zou, X. et al. 2015. Preparation and drug release behavior of pH-responsive bovine serum
574 albumin-loaded chitosan microspheres. *J Ind Eng Chem* 21, pp. 1389–1397.
575

Figure Legends

Figure 1. Schematic of Chitosan (CS)-based coatings that were prepared using EPD.

Figure 2. Pulsed ElectroMagnetic Field (PEMF) setup.

Figure 3. (a) SEM image of EPD of CS, (b,c) SEM images of EPD of CS/Ga composite coating ((b) [Gallium(III) nitrate hydrate] = 10 mg L^{-1} and (c) [Gallium(III) nitrate hydrate] = 100 mg L^{-1}), (d,e) corresponding X-ray map; (f,g) corresponding EDX spectrum.

Figure 4. (a) Effect of the Ga concentration in the suspension on the loading efficiency of the EPD process, (b) Release of Ga from the composite coatings; (●) [Gallium(III) nitrate hydrate] = 100 mg L^{-1} and (■) [Gallium(III) nitrate hydrate] = 10 mg L^{-1}, (c) Chitosan degradation test in PBS.

Figure 5. Weight loss of CS and CS/Ga composite coatings immersed in PBS (pH 7.4) at 37 °C containing 1.5 μg ml^{-1} lysozyme: (▲) CS, (■) [Gallium(III) nitrate hydrate] = 10 mg L^{-1}, (●) [Gallium(III) nitrate hydrate] = 100 mg L^{-1}.

Figure 6. Cell viability (% vs. control) of SAOS-2 cells cultured with coatings extracts as determined by a Alamar Blue ^{TM} assay ($p < 0.05$, indicated by *). For 50% and 10%: cultures diluted, 50% and 90% (w%), into fresh SAOS-2 media.

Figure 7. Crystal violet assay indicates in vitro biofilm viability for *S. epidermidis*, (a) after 24h and 3 days (3D) in comparison with control (CS) ($p < 0.05$, indicated by *) , (b) after 24h in different pH (all the absorbance values normalized with CS value at pH 7.3).

Figure 8. Crystal violet assay indicates in vitro biofilm viability for *S. aureus*, (a) after 24h and 3 days (3D) in comparison with control (CS) ($p < 0.05$, indicated by *) , (b) after 24h in different pH (all the absorbance values normalized with CS value at pH=7.3).

Figure 9. Total CFU of *S. epidermidis* incubated in LB medium, (planktonic cells).

Figure 10. Total CFU of bacteria cells incubated in LB medium for 24 h and then biofilm cells were detached from the coatings; (a) *S. epidermidis*, (b) *S. aureus*.

Figure 11. Representative VP-SEM images of the EPD CS/Ga coatings incubated with *S. epidermidis* for 24h, (a) pure CS, (b) CS/LGa composite coating ([Gallium(III) nitrate hydrate]= 10 mg L^{-1}) and (c) CS/HGa composite coating ([Gallium(III) nitrate hydrate]= 100 mg L^{-1}).

Figure 12. Representative VP-SEM images of the EPD CS/Ga coatings incubated with *S. aureus* for 24h, (a) pure CS, (b) CS/LGa composite coating ([Gallium(III) nitrate hydrate]= 10 mg L^{-1}) and (c) CS/HGa composite coating ([Gallium(III) nitrate hydrate]= 100 mg L^{-1}).

Figure 13. PEMF impact on biofilm viability of *S. epidermidis* strain 14990 in EPD CS/Ga composite orthopaedic coating; after 24h; (a) at low frequency, (b) at high frequency (all the absorbance values are normalized to no PEMF CS value).

Figure 14. PEMF impact on biofilm viability of *S. aureus* strain 12600 in EPD CS/Ga composite orthopaedic coating; after 24h; (a) at low frequency, (b) at high frequency (all the absorbance values are normalized to no PEMF CS value).

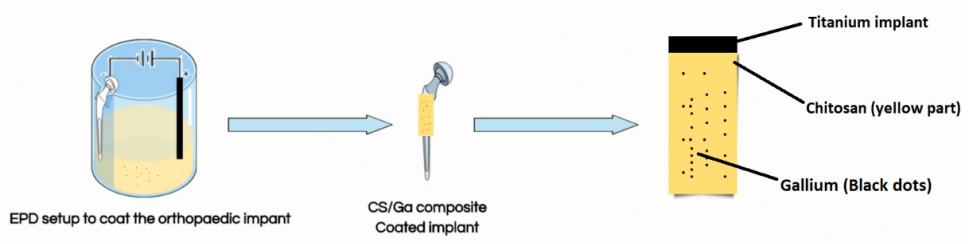

Figure 1. Schematic of Chitosan (CS)-based coatings that were prepared using EPD.

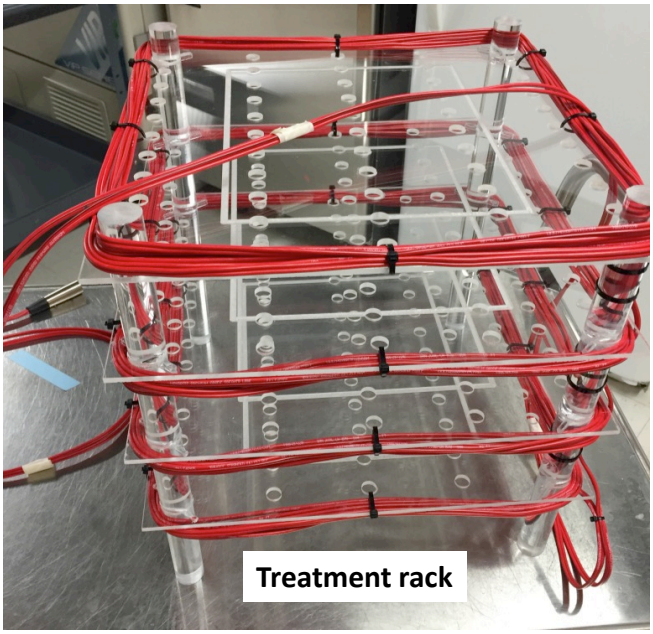

Figure 2. Pulsed ElectroMagnetic Field (PEMF) setup.

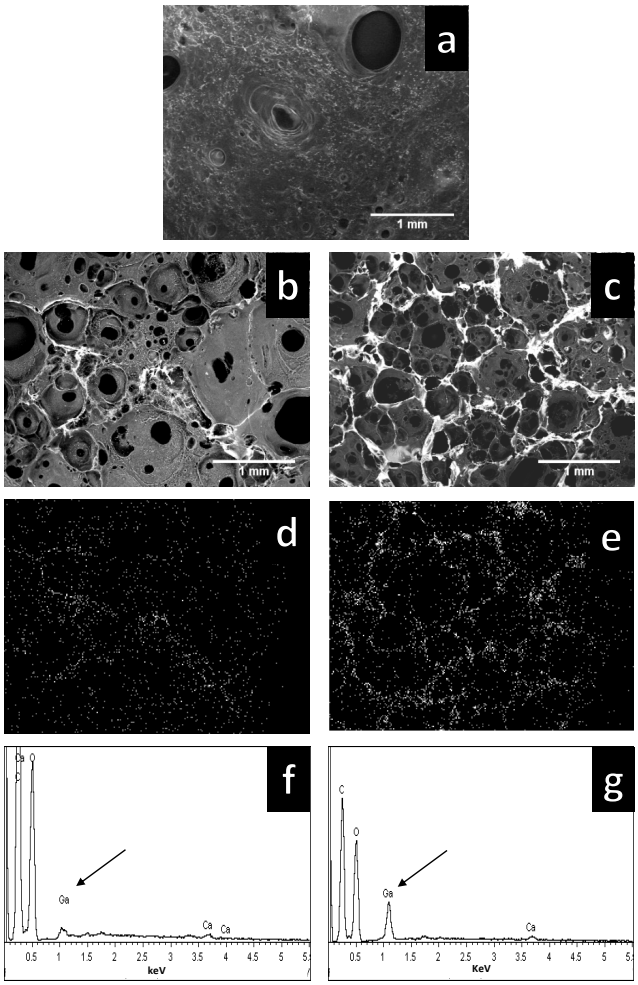

635

636 Figure 3. (a) SEM image of EPD of CS, (b,c) SEM images of EPD of CS/Ga composite coating

637 ((b) [Gallium(III) nitrate hydrate] = 10 mg L^{-1} and (c) [Gallium(III) nitrate hydrate] = 100 mg L^{-}

638 ^{1}), (d,e) corresponding X-ray map; (f,g) corresponding EDX spectrum.

639

a	[Ga]/[CS] in EPD bath (%)	[Ga]/[CS] in the coating (%)	Ga in the coating (mg)
LGa	0.27	0.18 ± 0.05	0.054
HGa	2.7	1.5 ± 0.08	0.34

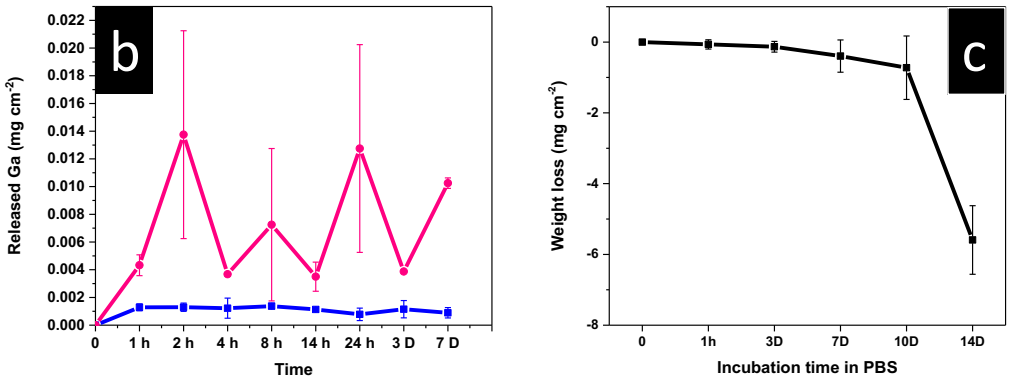

Figure 4. (a) Effect of the Ga concentration in the suspension on the loading efficiency of the EPD process, (b) Release of Ga from the composite coatings; (●) [Gallium(III) nitrate hydrate] = 100 mg L^{-1} and (■) [Gallium(III) nitrate hydrate] = 10 mg L^{-1}, (c) Chitosan degradation test in PBS.

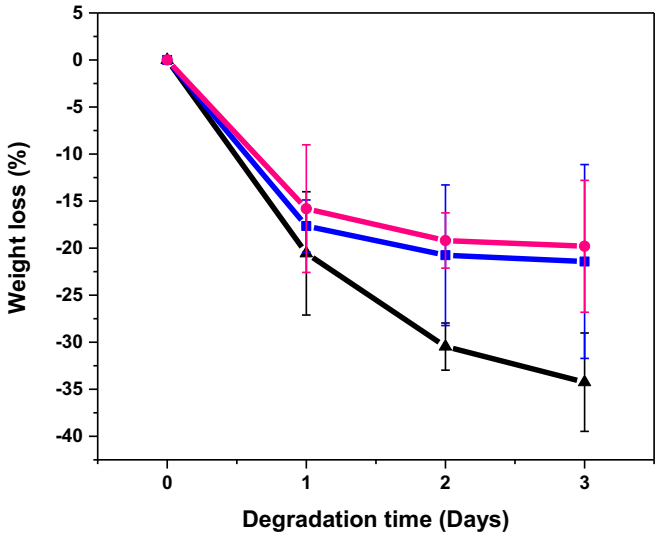

Figure 5. Weight loss of CS and CS/Ga composite coatings immersed in PBS (pH 7.4) at 37 °C containing 1.5 μg ml^{-1} lysozyme: (▲) CS, (■) [Gallium(III) nitrate hydrate] = 10 mg L^{-1}, (●) [Gallium(III) nitrate hydrate] = 100 mg L^{-1}.

676

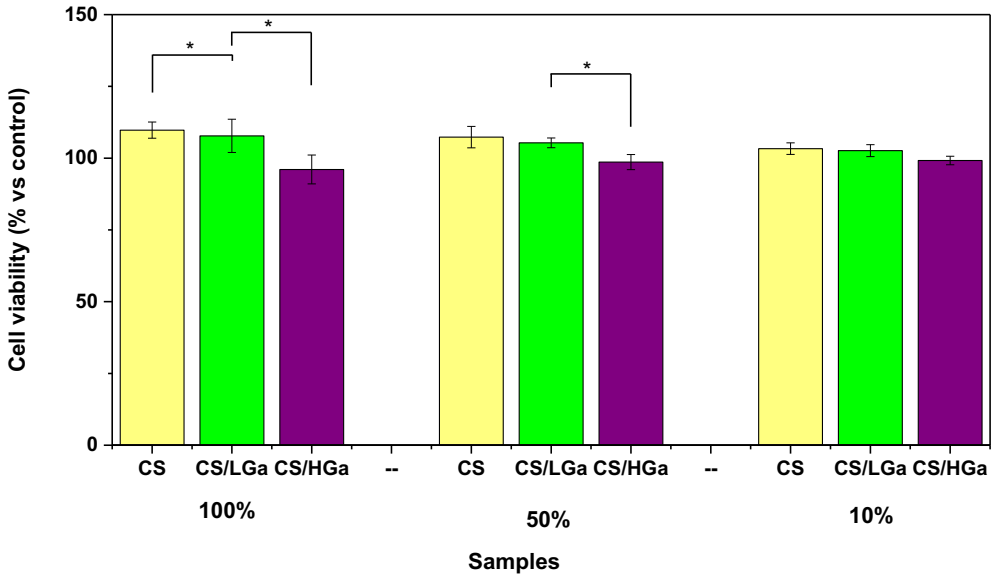

677

678 Figure 6. Cell viability (% vs. control) of SAOS-2 cells cultured with coatings extracts as

679 determined by a Alamar Blue ^{TM} assay ($p < 0.05$, indicated by *). For 50% and 10%: cultures

680 diluted, 50% and 90% (w%), into fresh SAOS-2 media.

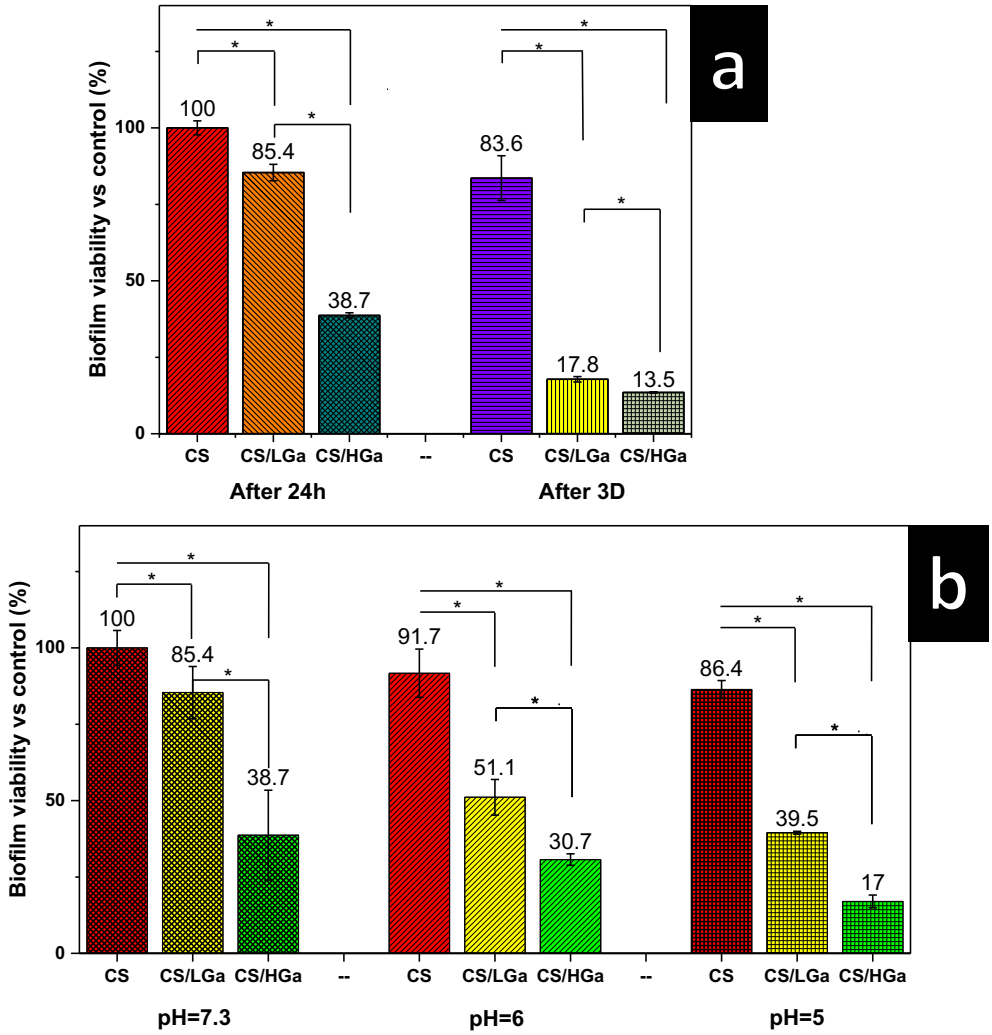

Figure 7. Crystal violet assay indicates in vitro biofilm viability for *S. epidermidis*, (a) after 24h and 3 days (3D) in comparison with control (CS) ($p < 0.05$, indicated by *) , (b) after 24h in different pH (all the absorbance values normalized with CS value at pH 7.3).

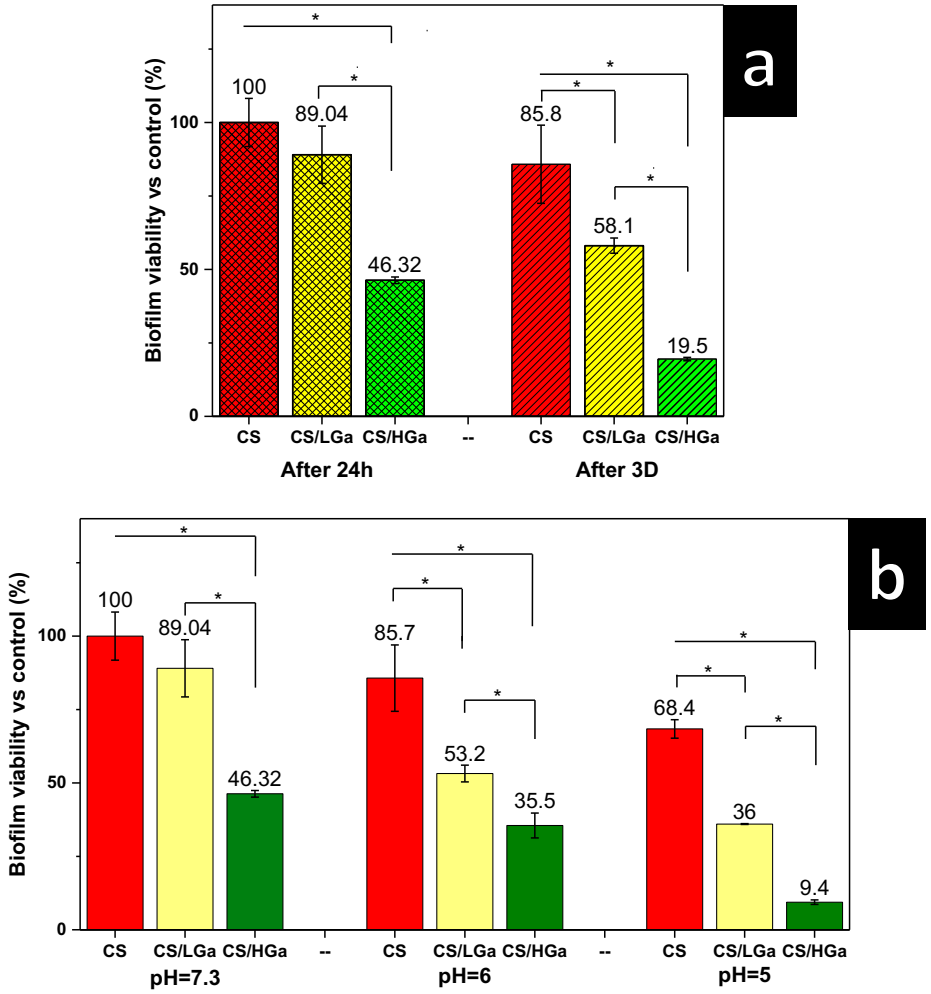

691

692 Figure 8. Crystal violet assay indicates in vitro biofilm viability for *S. aureus*, (a) after 24h and

693 3 days (3D) in comparison with control (CS) ($p < 0.05$, indicated by *) , (b) after 24h in different

694 pH (all the absorbance values normalized with CS value at pH=7.3).

695

696

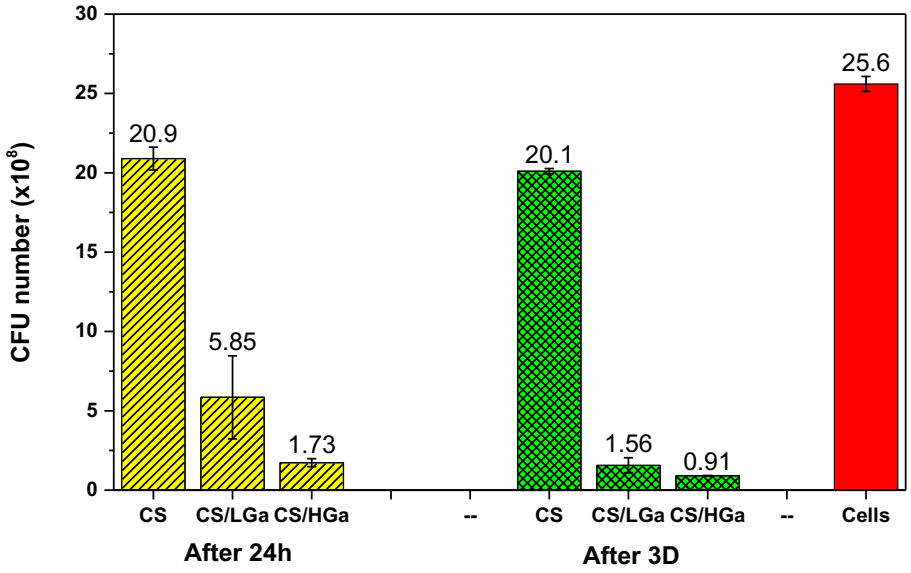

Figure 9. Total CFU of *S. epidermidis* incubated in LB medium, (planktonic cells).

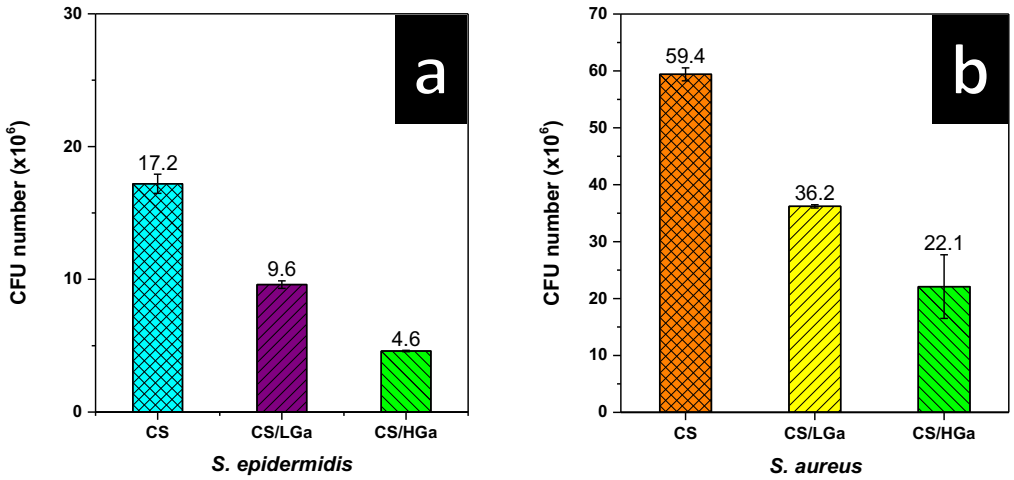

Figure 10. Total CFU of bacteria cells incubated in LB medium for 24 h and then biofilm cells were detached from the coatings; (a) *S. epidermidis*, (b) *S. aureus*.

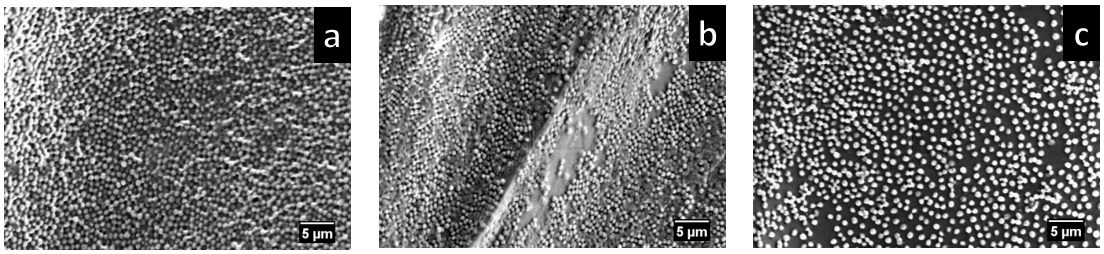

Figure 11. Representative VP-SEM images of the EPD CS/Ga coatings incubated with *S. epidermidis* for 24h, (a) pure CS, (b) CS/LGa composite coating ([Gallium(III) nitrate hydrate]= 10 mg L^{-1}) and (c) CS/HGa composite coating ([Gallium(III) nitrate hydrate]= 100 mg L^{-1}).

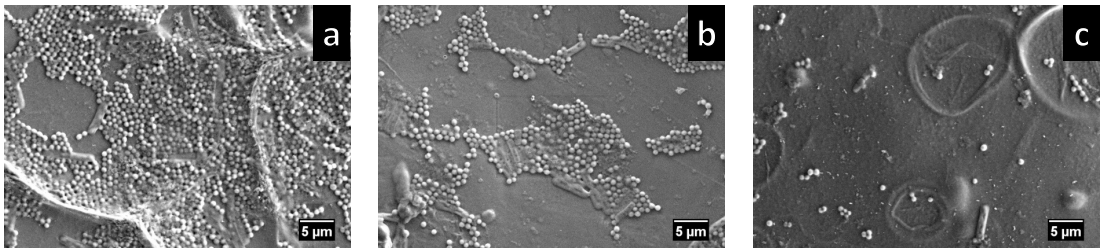

Figure 12. Representative VP-SEM images of the EPD CS/Ga coatings incubated with *S. aureus* for 24h, (a) pure CS, (b) CS/LGa composite coating ([Gallium(III) nitrate hydrate]= 10 mg L^{-1}) and (c) CS/HGa composite coating ([Gallium(III) nitrate hydrate]= 100 mg L^{-1}).

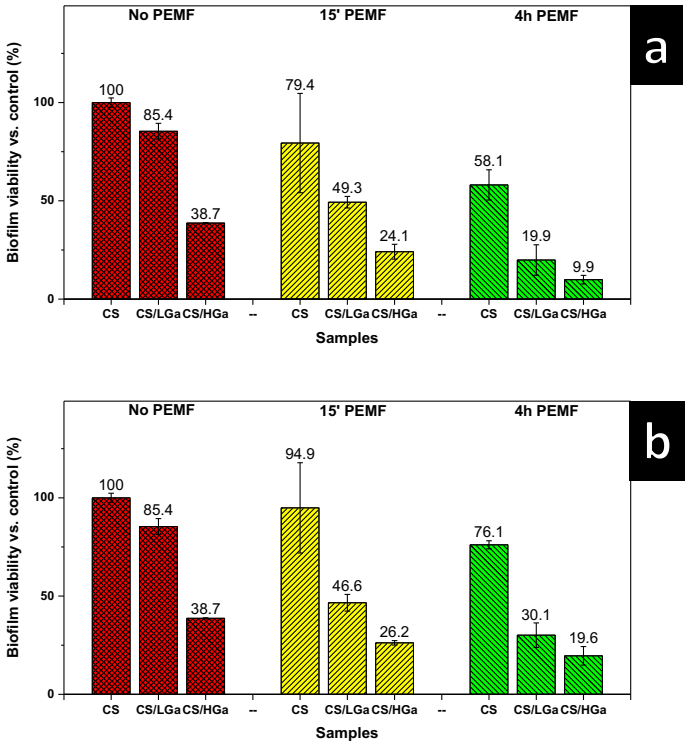

752

753 Figure 13. PEMF impact on biofilm viability of *S. epidermidis* strain 14990 in EPD CS/Ga
754 composite orthopaedic coating; after 24h; (a) at low frequency, (b) at high frequency (all the
755 absorbance values are normalized to no PEMF CS value).

756

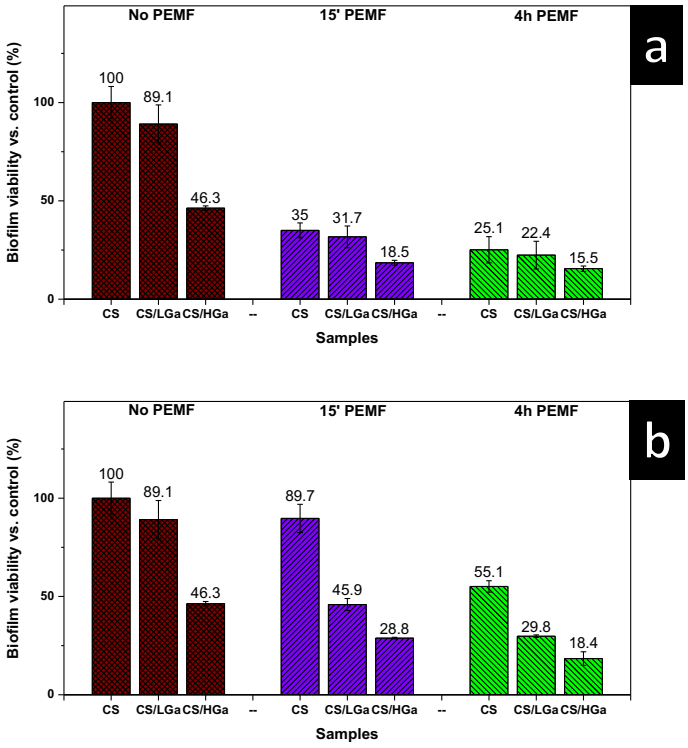

Figure 14. PEMF impact on biofilm viability of *S. aureus* strain 12600 in EPD CS/Ga composite orthopaedic coating; after 24h; (a) at low frequency, (b) at high frequency (all the absorbance values are normalized to no PEMF CS value).

Supporting information:

S.1 Electrophoretic deposition efficiency during Gallium-doped chitosan coatings fabrication

In the case of HGa (high gallium concentration):

We know that: $[Ga(NO_3)_3xH_2O]/[CS]=1/10$ and according to atomic weight:

$(Ga)/Ga(NO_3)_3xH_2O = 70/255.74 = 0.27$

Then: [Ga]/[CS]= 0.027 (2.7%) (Weight % of Ga in the deposition bath)

ICP result: 1.5 % (Weight % of deposited Ga in the scaffold)

Then: 1.5/2.7 = 55% (EPD Efficiency).

S.2 FTIR spectroscopy

Figure S.1 shows Fourier Transform Infrared (FTIR) spectra -obtained in transmission mode of CS film and CS/Ga composite films. The main peaks of chitosan can be detected in the spectra and are attributed to C=O stretching (amide I) at 1650 cm^{-1}, to N-H bending (amide II) at 1558 cm^{-1}, and to C-N stretching (amide III) at 1320 cm^{-1} (Leceta et al. 2013). By a qualitative analysis of the spectra, no peaks related to a chemical bond between chitosan and gallium, have been observed. This result highlights that gallium could be physically bonded to chitosan macromolecules (e.g., weak bonds) or entrapped into the chitosan macromolecules. In fact, Energy Dispersive X-ray (EDX) analyses performed on chitosan/Ga substrates prove the presence of gallium (Figure 2f – 2g) as well as the Inductive Coupled Plasma – Optical Emission Spectrometry (ICP-OES) investigation detects the Ga release from the prepared materials (Figure 4a).

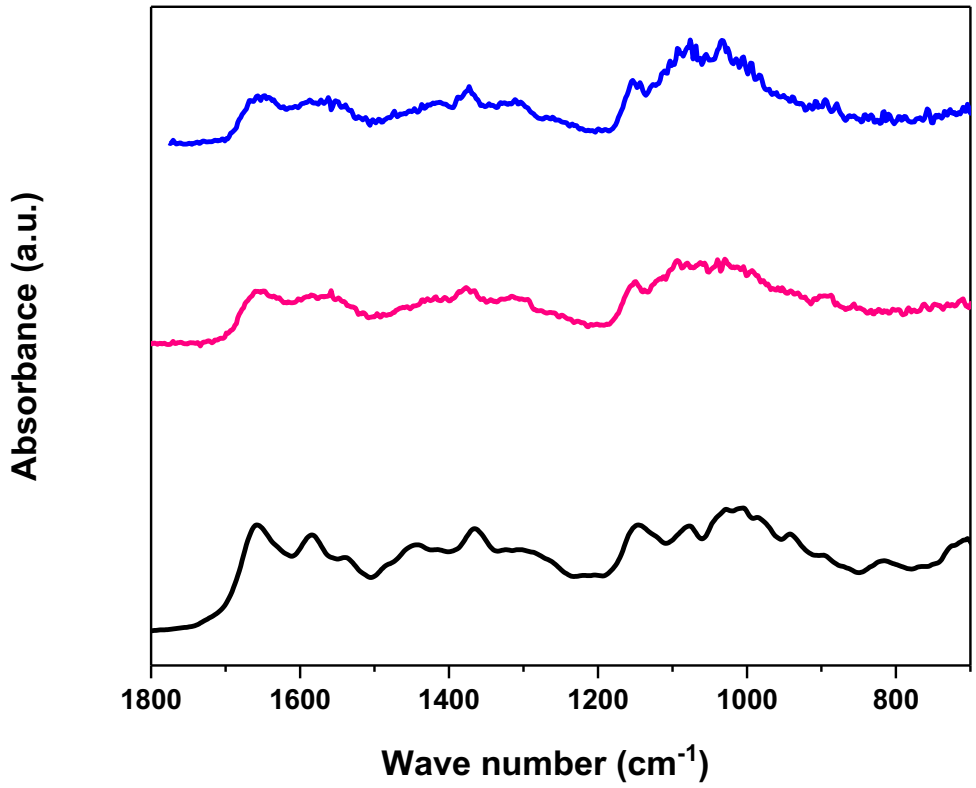

794

795 Figure S.1. Infrared spectra for CS and CS/Ga composite coatings, (−) CS, (−) [Gallium (III)

796 nitrate hydrate] = 10 mg L-1, (–) [Gallium (III) nitrate hydrate] = 100 mg L-1.

797